

Online Anomalous Subtrajectory Detection on Road Networks with Deep Reinforcement Learning

Qianru Zhang^{*†}, Zheng Wang^{††}, Cheng Long[†], Chao Huang^{*}, Siu-Ming Yiu^{*}, Yiding Liu[§],
Gao Cong[‡], Jieming Shi[¶]

^{*}Department of Computer Science, The University of Hong Kong, Hong Kong SAR

[‡]School of Computer Science and Engineering, Nanyang Technological University, Singapore, [§]Baidu Inc, China

[¶]Department of Computing, The Hong Kong Polytechnic University, Hong Kong SAR

{qrzhang,chuang,smyiu}@cs.hku.hk, zheng011@e.ntu.edu.sg, {c.long,gaocong}@ntu.edu.sg
liuyiding.tanh@gmail.com, jieming.shi@polyu.edu.hk

Abstract—Detecting anomalous trajectories has become an important task in many location-based applications. While many approaches have been proposed for this task, they suffer from various issues including (1) incapability of detecting anomalous subtrajectories, which are finer-grained anomalies in trajectory data, and/or (2) non-data driven, and/or (3) requirement of sufficient supervision labels which are costly to collect. In this paper, we propose a novel reinforcement learning based solution called **RL4OASD**, which avoids all aforementioned issues of existing approaches. **RL4OASD** involves two networks, one responsible for learning features of road networks and trajectories and the other responsible for detecting anomalous subtrajectories based on the learned features, and the two networks can be trained iteratively without labeled data. Extensive experiments are conducted on two real datasets, and the results show that our solution can significantly outperform the state-of-the-art methods (with 20-30% improvement) and is efficient for online detection (it takes less than 0.1ms to process each newly generated data point).

Index Terms—trajectory data, anomalous subtrajectory detection, road networks, deep reinforcement learning

I. INTRODUCTION

With the advancement of mobile computing and geographical positioning techniques, such as GPS devices and smart phones, massive spatial trajectory data is being generated by various moving objects (e.g., people, vehicles) in spatial spaces. Such collected trajectory data records the mobility traces of moving objects at different timestamps, which reflects diverse mobility patterns of objects. Accurate spatial trajectory data analysis serves as the key technical component for a wide spectrum of spatial-temporal applications, including intelligent transportation [1], location-based recommendation service [2], pandemic tracking [3], and crime prevention for public safety [4].

Among various trajectory mining applications, detecting anomalous trajectories plays a vital role in many practical scenarios. For example, the real-time vehicle trajectory anomaly detection is beneficial for better traffic management [5]. Additionally, studying the mobility behaviors of humans for discovering their anomalous trajectories is helpful for

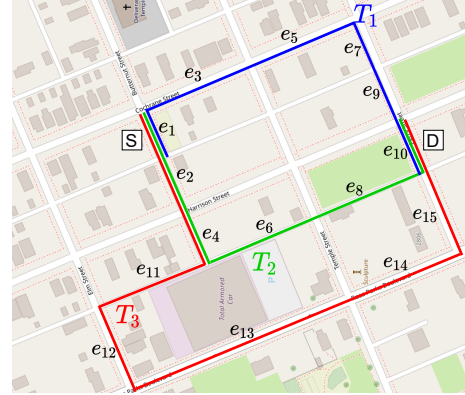


Fig. 1. An example of anomalous trajectory. T_1 , T_2 and T_3 are three trajectories from the same source e_1 to the same destination e_{10} .

predicting event outliers (e.g., civil unrest and pandemic outbreaks) [6]. In such context, an outlier/anomaly refers to a trajectory which does not show the normal mobility patterns and deviates from the majority of the trajectories with the same source and destination [7], [8] (termed as SD pair). Consider the example in Figure 1. There are three trajectories from the source $S(e_1)$ to the destination $D(e_{10})$. The trajectory T_3 (the red one) is considered as anomalous if the majority of the trajectories with the same SD pair $< S, D >$ follow either T_1 (the blue one) or T_2 (the green one).

Recently, detecting anomalous trajectories has attracted much attention, and many efforts have been devoted to proposing various methods ([8], [9], [10], [11], [12], [13]) for solving this problem. However, several key challenges have not been well addressed in current methods, which are summarized in Table I and elaborated as follows.

(1) **Incapability of detecting anomalous subtrajectories.** Most existing approaches [9], [10], [11], [12], [13] have only focused on identifying anomalous trajectories at coarse-grained levels, and detecting whether a trajectory as a whole is anomalous or not. However, the anomalous trajectory detection at the fine-grained level is more beneficial for better decision making in smart city applications, but unfortunately less explored in current methods. For instance,

[†]Equal contribution.

TABLE I
THE EXISTING METHODS AND THEIR CORRESPONDING ISSUES (✓ INDICATES
THE ISSUE EXISTS AND × OTHERWISE).

	Incapability of detecting anomalous subtrajectories	Non-data driven	Requirement of sufficient supervision labels
[8]	×	✓	×
[9]	✓	×	×
[10]	✓	✓	×
[11]	✓	×	×
[12]	✓	×	✓
[13]	✓	×	✓

a ride-hailing company can immediately spot an abnormal driver when his/her trajectory starts to deviate from the normal route, which indicates an anomalous *subtrajectory*. Hence, in this work, we propose to detect fine-grained anomalous subtrajectories in a timely manner.

(2) **Non-data driven.** Some existing approaches are based on pre-defined parameters and/or rules, and are not data driven [8], [10]. For example, the approach in [8] is to use some manually defined parameters to isolate an anomalous subtrajectory. It uses an adaptive window maintaining the latest incoming GPS points to compare against normal trajectories, where the normal trajectories are supported by the majority of the trajectories within an SD pair. As a new incoming point is added to window, it then checks the support of the subtrajectory in the window. If the support is larger than a pre-defined threshold, the point is labeled to be normal; otherwise, the point is labeled to be anomalous, and the adaptive window is reduced to contain only the latest point. The process continues until the trajectory is completed. The anomalous subtrajectory is recognized as those points labeled to be anomalous. However, the threshold is hard to set appropriately, and not general enough to cover all possible situations or adaptive to different road conditions. Another approach in [10] uses trajectory similarity (e.g., discrete Frechet) to detect anomalies. It computes the distance between a given normal trajectory and the current partial trajectory for each new incoming point, it reports an anomaly event if the distance exceeds a given threshold; otherwise, the detection continues.

(3) **Requirement of sufficient supervision labels.** While several machine learning models have been developed to identify the anomalous trajectories [12], [13], the effectiveness of those methods largely relies on sufficient labeled data under a supervised learning framework. Nevertheless, practical scenarios may involve a very limited amount of labeled anomalous trajectories compared with the entire trajectory dataset due to the requirement of heavy human efforts, e.g., the trajectory data used in [8] only contains 9 SD pairs.

In this paper, we propose a novel reinforcement learning based solution RL4OASD, which avoids the aforementioned issues of existing approaches. First, RL4OASD is designed to detect anomalous *subtrajectories* in an online fashion, and thus it avoids the first issue. It achieves this by predicting a normal/anomalous label for each road segment in a trajectory and detecting anomalous subtrajectories based on

the labels of road segments. Second, RL4OASD is a data-driven approach relying on data *without labels*, and thus it avoids the second and third issues. Specifically, RL4OASD consists of three components, namely data preprocessing, network RSRNet and network ASDNet (see Figure 2). In data preprocessing, it conducts map-matching on raw trajectories, mapping them onto road networks and obtains the map-matched trajectories. Based on the map-matched trajectories, it computes some labels of the road segments involved in trajectories using some heuristics based on the historical transition data among road segments. The labels, which are noisy, will be used to train RSRNet in a weakly supervised manner. In RSRNet, it learns the representations of road segments based on both traffic context features and normal route features. These representations in the form of vectors will be fed into ASDNet to define the states of a Markov decision process (MDP) for labeling anomalous subtrajectories. In ASDNet, it models the task of labeling anomalous subtrajectories as an MDP and learns the policy via a policy gradient method [14]. ASDNet outputs refined labels of road segments, which are further used to train RSRNet again, and then RSRNet provides better observations for ASDNet to train better policies. We emphasize that the noisy labels computed by the preprocessing component only provide some prior knowledge to address the cold-start problem of training RSRNet, but are not used to train the model as in a supervised paradigm. Furthermore, the concept of anomalous trajectory might drift over time. For example, due to some varying traffic conditions (e.g., some accidents), the trajectory might gradually deviate from a normal route, and the concept of “normal” and “anomalous” is changed accordingly. RL4OASD can handle “concept drift” with an online learning strategy, i.e., it continues to be refined when new data comes in.

Our contributions can be summarized as follows.

- We propose the first deep reinforcement learning based solution to detect anomalous subtrajectories. The proposed model 1) can detect anomalous subtrajectories naturally, 2) is data-driven, and 3) does not require labeled data. In addition, it can handle the concept drift of anomalous trajectories via online learning.
- We conduct extensive experiments on two real-world trajectory datasets, namely Chengdu and Xi’an. We compare our proposed solution with various baselines, and the results show that our solution is effective (e.g., it yields 20-30% improvement compared to the best existing approach) and efficient (e.g., it takes less than 0.1ms to process each newly generated data point).
- We manually label the anomalous subtrajectories for two real datasets, Chengdu and Xi’an, for testing. Each labeled dataset covers 200 SD pairs and 1,688 (resp. 1,057) map-matched trajectories with these SD pairs for the Chengdu dataset (resp. the Xi’an dataset). This labeled dataset is more than 50 times larger than the existing known dataset [8]. The manually labeled test

data is publicly accessible via the link ¹. We believe this relatively large labeled dataset would help with comprehensive and reliable evaluations on approaches for anomalous subtrajectory detection.

II. RELATED WORK

A. Online Anomalous Trajectory/Subtrajectory Detection.

Online anomalous trajectory detection aims to detect an ongoing trajectory in an online manner. Existing studies propose many methods for the problem and involve two categories: heuristic-based methods [8], [10] and learning-based methods [9], [11].

For heuristic methods, Chen et al. [8] investigate the detection of anomalous trajectories in an online manner via the isolation-based method, which aims to check which parts of trajectories are isolated from the reference (i.e., normal) trajectories with the same source and destination routes. This method aims to detect the anomalous subtrajectories from ongoing trajectories, which is similar to our paper. However, this method models reference trajectories based on many manually-set parameters. Besides, the performance of this method is evaluated on a small manually labeled dataset with 9 SD pairs only, which fails to reflect the generalization of this method. A recent work [10] proposes to calculate the trajectory similarity via discrete Frechet distance between a given reference route and the current partial route at each timestamp. If the deviation exceeds a given threshold at any timestamp, and the system alerts that an anomaly event of detouring is detected. There are many predefined parameters involved in this method. Our work differs from these heuristic-based studies in that it is based on a policy learned via reinforcement learning instead of the hand-crafted heuristic with many predefined parameters (e.g., the deviation threshold) for detecting anomalies. Besides, we evaluate the performance of our method on a large dataset.

For learning-based methods, a recent study [11] proposes to detect anomalous trajectories via a generation scheme, which utilizes the Gaussian mixture distribution to represent different kinds of normal routes and detects those anomalous trajectories that cannot be well-generated based on the given representations of normal routes. This method aims to detect whether the ongoing trajectory is anomalous or not. Another learning-based method [9] proposes a probabilistic model to detect trajectory anomalies via modeling the distribution of driving behaviours from historical trajectories. The method involves many potential features that are associated with driving behaviour modeling, including road level and turning angle, etc. This method also only targets whether the online trajectory is anomalous or not.

In our work, we target a finer-grained setting, i.e., detecting which part of an anomalous trajectory, namely subtrajectory, is responsible for its anomalousness in an online manner. Nevertheless, anomalous subtrajectory detection is not the focus in these studies.

¹<https://www.dropbox.com/sh/imix3otoep49v0g/AACQLPpgA0jMdTg7LV-GdL70a?dl=0>

B. Offline Anomalous Trajectory Detection.

Offline anomalous trajectory detection refers to detecting an anomalous trajectory or anomalous subtrajectories of a trajectory, where the trajectory inputted in an offline manner. Also, there are two types of studies. One type is heuristic-based methods [15], [16], [17], [18], [19] and another type is learning-based methods [20], [12]. For heuristic-based methods, some heuristic metrics involving distance or density metrics are usually utilized to detect anomalous trajectories. For example, an early study [15] proposes a partition and detect mechanism to conduct anomalous subtrajectory detection. The main idea is to partition the trajectories and detect the anomalous trajectory segments by computing the distance of each segment in a target trajectory to the segments in other trajectories. A recent study [18] utilizes edit distance metrics to detect anomalous trajectories based on mining the normal trajectory patterns. Another study [16] proposes to cluster trajectories based on the same itinerary and further detect anomalous trajectories via checking whether the target trajectory is isolated from the cluster. In addition, [21] proposes a system which is utilized to detect fraud taxi driving. The main idea of this method is to detect anomalous trajectories via combining distance and density metrics.

Other studies are proposed to detect anomalous trajectories with learning-based methods. For example, Song et al [12] adopt recurrent neural network (RNN) to capture the sequential information of trajectories for detection. However, the proposed model needs to be trained in a supervised manner, and the labeled data is usually unavailable in real applications. Another learning-based work [20] aims at detecting anomalous trajectories by new moving subjects (i.e., new taxi driver detection) with an adversarial model (i.e., GAN) is adapted. It is clear that these methods proposed in this line of research cannot be utilized for the online detection scenario.

C. Other Types of Anomalous Detection Studies.

Some works [19], [22], [23], [24] focus on other types of anomalous trajectory detection, which are related to ours. We review them as follows. Banerjee et al. [19] study temporal anomaly detection, which employs travel time estimation and traverses some potential subtrajectories in a target trajectory, where the anomalies are identified if the travel time largely deviates from the expected time. Li et al. [22] detect temporal anomalies and a method utilizing historical similarity trends is studied. In addition, Ge et al. [23] investigate the Top-K evolving anomalies and Yu et al. [24] detect anomalous trajectories in large-scale trajectory streams.

D. Deep Reinforcement Learning.

Deep reinforcement learning aims to guide an agent to make sequential decisions to maximize a cumulative reward [25], as the agent interacts with a specific environment, which is usually modeled as a Markov decision process (MDP) [26]. In recent years, reinforcement learning has attracted much research attention. For example, Oh et

al. [27] explores inverse reinforcement learning for sequential anomaly detection, and Huang et al. [28] designs a deep RL-based anomaly detector for time series detection. Wang et al. [29] proposes to use RL-based algorithms to accelerate subtrajectory similarity search. In this paper, we propose a novel RL-based solution for online anomalous subtrajectory detection (called RL4OASD), and a policy gradient method [30] is adopted for solving the problem. To our best knowledge, this is the first deep reinforcement learning based solution for online anomalous subtrajectories detection.

III. PRELIMINARIES AND PROBLEM STATEMENT

A. Preliminaries

Raw Trajectory. A raw trajectory T consists of a sequence of GPS points, i.e., $T = \langle p_1, p_2, \dots, p_n \rangle$, where a GPS point p_i is in the form of a triplet, i.e., $p_i = (x_i, y_i, t_i)$, meaning that a moving object is located on (x_i, y_i) at timestamp t_i , and n represents the length of the trajectory T .

Road Network. A road network is represented as a directed graph $G(V, E)$, where V represents a vertex set referring to crossroads or intersections, and E represents an edge set referring to road segments, and for each edge e , it connects two vertexes u and v on the road network, denoted as $e = (u, v)$.

Map-matched Trajectory. A map-matched trajectory refers to a trajectory generated by a moving object on road networks, which corresponds to a sequence of road segments [31], i.e., $T = \langle e_1, e_2, \dots, e_n \rangle$.

For simplicity, we use T to denote a map-matched trajectory, and we refer to map-matched trajectories as trajectories or routes interchangeably in the rest of the paper.

Subtrajectory and Transition. A subtrajectory $T[i, j]$ corresponds to a portion of the trajectory $T = \langle e_1, e_2, \dots, e_n \rangle$ from e_i to e_j , $1 \leq i \leq j \leq n$. A transition is defined as a special case of a subtrajectory, which only consists of two adjacent road segments, i.e., $\langle e_{i-1}, e_i \rangle$, where $1 < i \leq n$.

B. Problem Definition

We study the problem of *online anomalous subtrajectory detection*. Consider a source S and destination D pair (SD pair) and a set of trajectories \mathcal{T} between them. Intuitively, a trajectory T can be considered as *normal* if it follows the route traveled by the majority of trajectories in \mathcal{T} . Based on this, we denote an *anomalous* subtrajectory representing a part of a trajectory, which *does not* follow the normal routes within the SD pair. We formulate the problem as follows.

Problem 1 (OASD): Given an ongoing trajectory $T = \langle e_1, e_2, \dots, e_n \rangle$ that is generated from its source S_T to destination D_T in an online fashion, where the points e_i are generated one by one, and the future points are not accessible in advance. The OASD problem is to detect and update which parts of T (i.e., subtrajectories) are anomalous, while T is sequentially generated.

IV. METHODOLOGY

A. Overview of RL4OASD

Determining whether a subtrajectory of an ongoing trajectory is anomalous or not is a decision-making process, which could be modeled as a Markov decision process (MDP) [26]. We propose a weakly supervised framework called RL4OASD (see Figure 2 for an overview). The framework consists of three components, namely data preprocessing (Section IV-B), RSRNet (Section IV-C) and ASDNet (Section IV-D).

In data preprocessing, we conduct map-matching on raw trajectories, mapping them onto road networks and obtain the map-matched trajectories. Based on the map-matched trajectories, we compute some labels of the road segments involved in trajectories using some heuristics based on the historical transition data among road segments. The labels, which are noisy, will be used to train RSRNet in a weakly supervised manner. In RSRNet, we learn the representations of road segments based on both traffic context features and normal route features. These representations in the form of vectors will be fed into ASDNet to define the states of the MDP for labeling anomalous subtrajectories. In ASDNet, we model the task of labeling anomalous subtrajectories as a MDP and learn the policy via a policy gradient method [14]. ASDNet outputs refined labels of road segments, which are further used to train RSRNet again, and then RSRNet provides better observations for ASDNet to train better policies. The process iterates and we call the resulting algorithm combining RSRNet and ASDNet as RL4OASD (Section IV-E).

We explain some insights behind the effectiveness of RL4OASD as follows. First, in RSRNet, both traffic context features (e.g., driving speed, trip duration) and normal route features that are associated with the anomalies are well captured into the model. Second, in ASDNet, the task of labeling anomalous subtrajectories is formulated as a MDP, whose policy is learned in a data-driven manner, instead of using heuristics (e.g., some pre-defined parameters) as the existing studies do. Third, RSRNet is first trained with noisy labels for dealing with the cold-start problem. Then, RSRNet and ASDNet are trained iteratively and collaboratively, where RSRNet uses ASDNet's outputs as labels and ASDNet uses the outputs of RSRNet as features.

B. Data Preprocessing

The data processing component involves a map matching process [31] and a process of obtaining noisy labels. The latter produces some noisy labels, which will be utilized to pre-train the representations in RSRNet and also to provide a warm-start for the policy learning in ASDNet. Recall that we do not assume the availability of real labels for training since manually labeling the data is time-consuming. Specifically, the process of obtaining noisy labels involves four steps.

Step-1: We group historical trajectories in a dataset with respect to different SD pairs and time slots. Here, we have 24 time slots if we partition one day with one hour granularity,

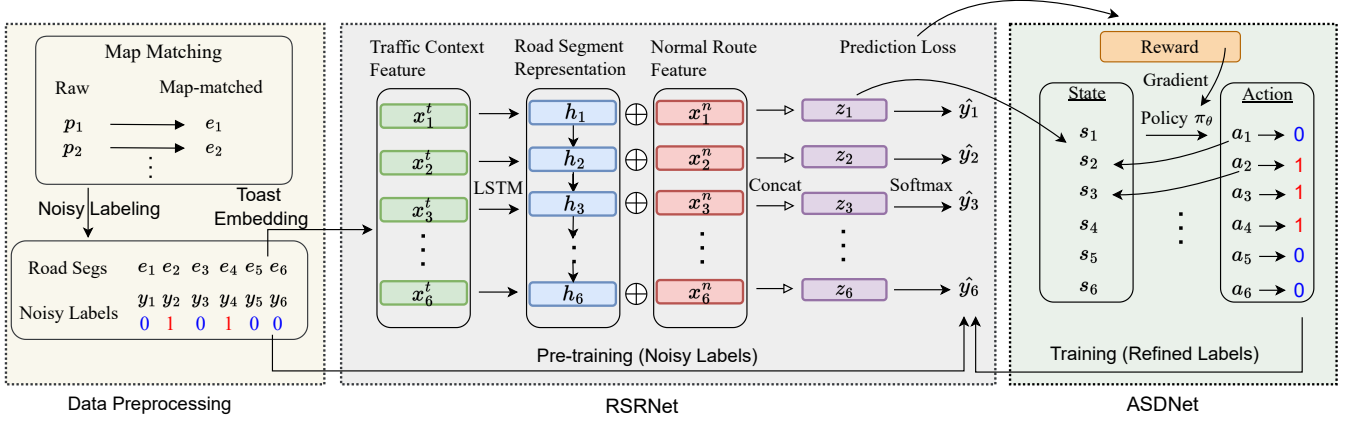


Fig. 2. Overview of RL4OASD, where \oplus denotes the concatenation operation.

and we say a trajectory falls into a time slot if its starting travel time is within the slot. For example, in Figure 1, we have three map-matched trajectories T_1 , T_2 and T_3 with the source e_1 and destination e_{10} . Assuming the starting travel times of T_1 , T_2 and T_3 are 9:00, 9:10, and 9:30, respectively. Then, all three trajectories are in the same group because they are within the same time slot with one hour granularity.

Step-2: We then compute the fraction of *transitions* each from a road segment to another with respect to all trajectories in each group. Suppose that there are 5 trajectories traveling along T_1 , 4 along T_2 , and only 1 along T_3 , the fraction of *transition* $< e_1, e_2 >$ is calculated as $5/10 = 0.5$ since it appears 5 times (along T_2 and T_3) in all 10 trajectories.

Step-3: For each trajectory, we refer to the group it belongs to and map it to a sequence of *transition* fractions with respect to each road segment. For example, for a trajectory traveling the route as T_3 , its mapped *transition* sequence is $< *, e_1 >, < e_1, e_2 >, < e_2, e_4 >, < e_4, e_{11} >, < e_{11}, e_{12} >, < e_{12}, e_{13} >, < e_{13}, e_{14} >, < e_{14}, e_{15} >, < e_{15}, e_{10} >$, where we pad the initial transition as $< *, e_1 >$, and the corresponding fraction sequence is $< 1.0, 0.5, 0.5, 0.1, 0.1, 0.1, 0.1, 0.1, 1.0 >$. Note that the fractions on the source e_1 (corresponding to $< *, e_1 >$) and the destination e_{10} (corresponding to $< e_{15}, e_{10} >$) are always set to 1.0, since the source and destination road segments are definitely travelled within its group.

Step-4: We obtain the noisy labels by using a threshold parameter α , where 0 denotes a normal road segment, whose fraction is larger than α meaning that the road segment is frequently traveled, and 1 otherwise. For example, by using the threshold $\alpha = 0.5$, we obtain the noisy labels of T_3 as $< 0, 1, 1, 1, 1, 1, 1, 1, 0 >$.

C. Road Segment Representation Network (RSRNet)

In RSRNet, we adopt the LSTM [32] structure, which accepts trajectories with different lengths and captures the sequential information behind trajectories. We embed two types of features into representations, namely the traffic context features on road networks and the normal route features for a given SD pair.

Traffic Context Feature (TCF). A map-matched trajectory corresponds to a sequence of road segments and each road segment is naturally in the form of a token (i.e., the road segment id). We pre-train each road segment in the embedding layer of RSRNet as a vector, which captures traffic context features (e.g., driving speed, trip duration, road type). To do this, we employ Toast [33], which is a recent road network representation learning model to support road segment based applications. The learned road segment representations will be used to initialize the embedding layer in RSRNet, and those embeddings can be further optimized with the model training. Other road network representation models [34], [35] are also applicable for the task.

Normal Route Feature (NRF). Given an SD pair in a time slot, we first infer the normal routes within it. Intuitively, the normal trajectories often follow the same route. If a trajectory contains some road segments that are rarely traveled by others, it probably contains anomalies. Therefore, we infer a route as the normal route by calculating the fraction of the trajectories passing through the route with respect to all trajectories within its SD pair. The inferred results are obtained via comparing a threshold (denoted by δ) with the fraction of each road segment, i.e., a route is inferred as the normal if the fraction is larger than the threshold, and vice versa. For example, in Figure 1, recall that there are 5 trajectories traveling along T_1 , 4 along T_2 , and only 1 along T_3 . Given $\delta = 0.3$, we infer T_1 (and resp. T_2) as the normal route, because its fraction $5/10 = 0.5$ (and resp. $4/10 = 0.4$) is larger than the threshold δ in all 10 trajectories. Based on the inferred normal routes, we then extract the features of a trajectory. For example, given a trajectory following T_3 , we extract the features as follows: a road segment in a target trajectory is normal (i.e., 0) if the transition on that road segment occurs in the inferred normal routes; and 1 otherwise. For example, the extracted normal features of T_3 are $< 0, 0, 0, 1, 1, 1, 1, 1, 0 >$, where the feature on the road segment e_2 is 0 since the transition $< e_1, e_2 >$ occurs in the normal route T_2 . Note that the source and destination road segments always have the feature 0 (i.e., normal). We notice normal route features and noisy

labels are both in the form of 0-1. The difference between them is that the former is to capture the information of normal routes, and correspondingly it is obtained by normal routes at a route-level. In contrast, the latter is used as the labels for training RSRNet, which is obtained by computing transition frequencies at an edge-level. In addition, the former is utilized during the whole training process, while the latter is utilized to pre-train the representations in RSRNet only (which would provide a warm-start for ASDNet). After obtaining the normal route features that are in the form of tokens, we then obtain a vector for the feature by embedding the tokens as one-hot vectors. We call the obtained vectors embedded normal route features.

Training RSRNet. Figure 2 illustrates the architecture of RSRNet. In particular, given a sequence of embedded traffic context features \mathbf{x}_i^t ($1 \leq i \leq n$), where n denotes the trajectory length, the LSTM obtains the hidden state \mathbf{h}_i at each road segment. We then concatenate \mathbf{h}_i with the embedded normal route feature \mathbf{x}_i^n , denoted by $\mathbf{z}_i = [\mathbf{h}_i; \mathbf{x}_i^n]$. Note that the two parts \mathbf{h} and \mathbf{x}^n capture the sequential trajectory information and normal route information, respectively. Note that we do not let \mathbf{x}^n go through the LSTM since it preserves the normal route feature at each road segment. We adopt cross-entropy loss to train RSRNet between the predicted label \hat{y}_i based on the \mathbf{z}_i and the noisy/refined label y_i , i.e.,

$$\mathcal{L} = \frac{1}{n} \sum_{i=1}^n \mathcal{H}(y_i, \hat{y}_i), \quad (1)$$

where \mathcal{H} denotes the cross-entropy operator.

D. Anomalous Subtrajectory Detection Network (ASDNet)

Consider the task of online anomalous subtrajectory detection is to sequentially scan an ongoing trajectory, and for each road segment, decide whether an anomaly happened at that position. This motivates us to model the process as a Markov decision process (MDP), involving states, actions, and rewards.

States. We denote the state when scanning the road segment e_i as \mathbf{s}_i . The state \mathbf{s}_i ($1 < i \leq n$) is represented as the concatenation of \mathbf{z}_i and $\mathbf{v}(e_{i-1}.l)$, i.e., $\mathbf{s}_i = [\mathbf{z}_i; \mathbf{v}(e_{i-1}.l)]$, where \mathbf{z}_i is obtained from RSRNet and $\mathbf{v}(e_{i-1}.l)$ denotes a vector of the label on the previous road segment e_{i-1} by embedding its token (i.e., 0 or 1). The rationale for the state design is to capture the features from three aspects, i.e., traffic context, normal routes and the previous label.

Actions. We denote an action of the MDP by a , which is to label each road segment as normal or not. Note that an anomalous subtrajectory boundary can be identified when the labels of two adjacent road segments are different.

Rewards. The reward involves two parts. One is called *local reward*, which aims to capture the local continuity of labels of road segments. The rationale is that the labels of normal road segments or anomalous road segments would not change frequently. The second one is called *global reward*, which aims to indicate the quality of the refined labels (indicated by

the cross-entropy loss of RSRNet). We take the loss as some feedback to guide the training of ASDNet.

The local reward is an intermediate reward, which encourages the continuity of the labels on road segments. Specifically, it is defined as

$$r_i^{local} = \text{sign}(e_{i-1}.l = e_i.l) \cdot \cos(\mathbf{z}_{i-1}, \mathbf{z}_i), \quad (2)$$

where the $\text{sign}(e_{i-1}.l = e_i.l)$ returns 1 if the condition $e_{i-1}.l = e_i.l$ is true (i.e., the labels are continued) and -1 otherwise; $\cos(\mathbf{z}_{i-1}, \mathbf{z}_i)$ denotes the cosine similarity between \mathbf{z}_{i-1} and \mathbf{z}_i , which are obtained from RSRNet. We choose the cosine similarity because it outputs a normalized value between 0 and 1, which corresponds to the same output range (i.e., between 0 and 1) of the global reward.

The global reward is designed to measure the quality of refined labels by ASDNet. We feed the refined labels into RSRNet, and compute the global reward as

$$r^{global} = \frac{1}{1 + \mathcal{L}}, \quad (3)$$

where \mathcal{L} denotes the cross-entropy loss in Equation 1. We notice this reward has the range between 0 and 1, and makes the objective of RSRNet well aligned with ASDNet (a smaller loss \mathcal{L} means a larger global reward).

Policy Learning on the MDP. The core problem of a MDP is to learn a policy, which guides an agent to choose actions based on the constructed states such that the cumulative reward, denoted by R_n , is maximized. We learn the policy via a policy gradient method [14], called the REINFORCE algorithm [36]. To be specific, let $\pi_\theta(a|s)$ denote a stochastic policy, which is used to sample an action a for a given state s via a neural network, whose parameters are denoted by θ . Then, the gradients of some performance measure $J(\theta)$ wrt the network parameters θ are estimated as

$$\nabla_\theta J(\theta) = \sum_{i=2}^n R_n \nabla_\theta \ln \pi_\theta(a_i | \mathbf{s}_i), \quad (4)$$

which can be optimized using an optimizer (e.g., Adam stochastic gradient ascent). The expected cumulative reward R_n for a trajectory is defined as

$$R_n = \frac{1}{n-1} \sum_{i=2}^n r_i^{local} + r^{global}. \quad (5)$$

Joint Training of RSRNet and ASDNet. We jointly train the two networks (e.g., RSRNet and ASDNet). First, we map raw trajectories on road networks and generate the noisy labels as explained in Section IV-B. Then, we randomly sample 200 trajectories to pre-train the RSRNet and ASDNet, separately. In particular, for the RSRNet, we train the network in a supervised manner with the noisy labels. For the ASDNet, we specify its actions as the noisy labels, and train the policy network via a gradient ascent step as computed by Equation 4. The pre-training provides a warm-start for the two networks, where the parameters of the two

Algorithm 1: The RL4OASD algorithm

Input: A map-matched trajectory

$T = \langle e_1, e_2, \dots, e_n \rangle$ which is inputted in an online manner

```
1 for  $i = 1, 2, \dots, n$  do
2   if  $i = 1$  or  $i = n$  then
3      $e_i.l \leftarrow 0$ ;
4   else
5     Call RSRNet for obtaining a representation  $\mathbf{z}_i$ ;
6     Construct a state  $\mathbf{s}_i = [\mathbf{z}_i; \mathbf{v}(e_{i-1}.l)]$ ;
7     Sample an action (i.e., 0 or 1),  $a_i \sim \pi_\theta(a|\mathbf{s})$ ;
8      $e_i.l \leftarrow a_i$ ;
9     Monitor the anomalous subtrajectory
      consisting of the road segments with the label
      1 and return the subtrajectory when it is
      formed;
10 end
11 Return a NORMAL trajectory signal;
```

networks have incorporated some information captured from the normal routes before joint training.

During the joint training, we randomly sample 10,000 trajectories, and for each trajectory, we generate 5 epochs to iteratively train the RSRNet and ASDNet. In particular, we apply the learned policy from ASDNet to obtain refined labels, and the refined labels are used to train the RSRNet to obtain the better representation \mathbf{z}_i on each road segment. Then, \mathbf{z}_i is used to construct the state to learn a better policy in ASDNet. Since the learned policy can further refine the labels, and the two networks are jointly trained with the best model is chosen during the process.

E. The RL4OASD Algorithm

Our RL4OASD algorithm is based on the learned policy for detecting anomalous subtrajectories. The process is presented in Algorithm 1. Specifically, RL4OASD accepts an ongoing trajectory in an online fashion for labeling each road segment as the normal (i.e., 0) or not (i.e., 1) (lines 1-9). It first labels the source or destination road segment as normal by definitions (lines 2-3). It then constructs a state via calling RSRNet (lines 5-6), and samples an action to label the road segment based on the learned policy in ASDNet (lines 7-8). It monitors the anomalous subtrajectory that involves the abnormal labels (i.e., 1) on the road segments and returns it when it is formed (line 9). Finally, if no anomaly is detected, the algorithm returns a NORMAL trajectory signal (line 11). We further develop two enhancements for boosting the effectiveness and efficiency of RL4OASD. One is called Road Network Enhanced Labeling (RNEL), and the other is called Delayed Labeling (DL).

Road Network Enhanced Labeling. For the RNEL, we utilize the graph structure of a road network to help labeling a road segment, where a label on a road segment is deterministic in one of three cases: (1) If $e_{i-1}.out = 1$, $e_i.in = 1$,

then $e_i.l = e_{i-1}.l$. (2) If $e_{i-1}.out = 1$, $e_i.in > 1$ and $e_{i-1}.l = 0$, then $e_i.l = 0$. (3) If $e_{i-1}.out > 1$, $e_i.in = 1$ and $e_{i-1}.l = 1$, then $e_i.l = 1$. Here, $e_i.out$ and $e_i.in$ denote the out degree and in degree of a road segment e_i , respectively, and $e_i.l$ denotes the label of the road segment e_i . The common intuition behind them is that: (a) any change of the anomalousness status from normal (0) at e_{i-1} to abnormal (1) at e_i means that there exist alternative transitions from e_{i-1} to other road segments (i.e., $e_{i-1}.out > 1$); and (b) any change of the anomalousness status from abnormal (1) at e_{i-1} to normal (0) at e_i means that there exist alternative transitions from other road segments to e_i (i.e., $e_i.in > 1$). Based on the rules, we only perform actions in the otherwise cases via the RL model, and some potential wrong decisions can therefore be avoided. In addition, the efficiency can be improved since the time of taking actions in some cases is saved via checking the rules instead of calling the RL model.

Delayed Labeling. For the DL, RL4OASD forms an anomalous subtrajectory whenever its boundary is identified, i.e., the boundary is identified at e_{i-1} if $e_{i-1}.l = 1$ and $e_i.l = 0$. Intuitively, it looks a bit rush to form an anomalous subtrajectory and may produce many short fragments from a target trajectory. Therefore, we consider a delay technique as a post-processing step. Specifically, it scans D more road segments that follow e_{i-1} when forming an anomalous subtrajectory. Among the D road segments, we choose the final position j ($i-1 < j \leq i-1+D$) where the road segment is with label 1, and then convert some 0's to 1's between the position $i-1$ and j . It could be verified the labeling with delay does not incur much time cost, and offers a better continuity to avoid forming too many fragments.

Time complexity. The time complexity of the RL4OASD algorithm is $O(n)$, where n denotes the length of a target trajectory. The time is dominated by two networks, i.e., RSRNet and ASDNet. We analyze them as follows. In RSRNet, the time cost for one road segment consists of (1) that of obtaining embeddings of TCF and NRF, which are both $O(1)$ and (2) that of obtaining the \mathbf{z} via a classic LSTM cell, which is $O(1)$. In ASDNet, the time cost for one road segment consists of (1) that of constructing a state, where the part \mathbf{z} has been computed in RSRNet and the part $\mathbf{v}(e.l)$ is obtained via an embedding layer, which is $O(1)$ and (2) that of sampling an action via the learned policy, which is $O(1)$. As we can see in Algorithm 1, the two networks are called at most n times. Therefore, the time complexity of the RL4OASD is $O(n) \times O(1) = O(n)$. We note that the $O(n)$ time complexity maintains the current best time complexity as those of existing algorithms [8], [9], [11] for the trajectory or subtrajectory anomaly detection task, and can largely meet practical needs for online scenarios as shown in our experiments.

Handling Concept Drift of Anomalous Trajectories. As discussed in Section III, we detect anomalous subtrajectories that do not follow the normal routes. However, the concept of “normal” and “anomalous” may change over time with

varying traffic conditions. For example, when some popular route is congested, then drivers may gradually prefer to travel another unpopular route (i.e., to avoid traffic jams). In this case, the unpopular route should be considered as a normal route, while the trajectories traveling the previous route may become anomalous. To handle the issue caused by the concept drift of the normal and anomalous, we adopt an online learning strategy [11], where the model continues to train with newly recorded trajectory data, and keeps its policy updated for the current traffic condition (we have validated the effectiveness of the strategy in Section V-G).

Discussion on the cold-start problem. As the anomalous subtrajectories are defined as unpopular parts, and thus there may exist a cold-start problem for the detection, where the historical trajectories are not sufficient for some SD pairs. Our method relies on the historical trajectories for defining the normal route feature. The feature is calculated as a relative fraction between 0 and 1. Specifically, the feature of a route is defined to be the number of trajectories along the route over the total number of trajectories within the SD pair. We have conducted experiments by varying the number of historical trajectories within the SD pairs in Table IX. The results show that our model is robust against sparse data, e.g., its effectiveness only degrades by 6% even if 80% of historical trajectories are dropped. The cold-start problem in anomalous trajectory/subtrajectory detection looks very interesting. We believe that some generative methods, e.g., to generate some routes within the sparse SD pairs, can possibly be leveraged to overcome the issue, which we plan to explore as future work.

V. EXPERIMENTS

A. Experimental Setup

Dataset. The experiments are conducted on two real-world taxi trajectory datasets from DiDi Chuxing ², namely *Chengdu* and *Xi'an*. All raw trajectories are preprocessed to map-matched trajectories via a popular map-matching algorithm [31], and the road networks of the two cities are obtained from OpenStreetMap ³. Following previous studies [11], [8], we preprocess the datasets and filter those SD-pairs that contain less than 25 trajectories to have sufficient trajectories to indicate the normal routes. We randomly sample 10,000 trajectories from the datasets for training, and the remaining for testing.

Ground Truth. By following the previous works [16], [8], [18], we manually label the anomalous subtrajectories, and take the labeled subtrajectories as the ground truth for the evaluation. Specifically, we sample 200 SD pairs with sufficient trajectories between them (e.g., at least 30 trajectories for each pair, and over 900 trajectories on average). For labeling subtrajectories, we illustrate all routes (i.e., map-matched trajectories) within each SD pair and highlight the road segments that are traveled by the majority of trajectories

TABLE II
DATASET STATISTICS.

Dataset	Chengdu	Xi'an
# of trajectories	677,492	373,054
# of segments	4,885	5,052
# of intersections	12,446	13,660
# of labeled routes (trajs)	1,688 (558,098)	1,057 (163,027)
# of anomalous routes (trajs)	1,436 (3,930)	813 (2,368)
Anomalous ratio	0.7%	1.5%
Sampling rate	2s \sim 4s	2s \sim 4s

as shown in Figure 5. We invite 5 participants, and first spend 10 minutes to get everyone to understand the visualization, then let them identify whether the routes are anomalous or not based on visual inspection. If a participant thinks the route is anomalous, we then ask the participant to label which parts are responsible for its anomalousness. For quality control, we randomly pick 10% trajectories, ask 5 other checkers to label these trajectories independently, adopt the majority voting to aggregate the labels, and compute the accuracy of the labels by the labelers against the aggregated ones by the checkers. The accuracy is 98.7% for Chengdu and 94.3% for Xi'an, which shows that our labeled datasets are with high accuracy.

Multiple raw trajectories may correspond to the same route and thus we have fewer routes than raw trajectories. We label 1,688 (resp. 1,057) routes, which correspond to 558,098 (resp. 163,027) raw trajectories before map-matching for Chengdu (resp. Xi'an). Among them, 1,436 (resp. 813) routes that correspond to 3,930 (resp. 2,368) raw trajectories are identified as the anomalous for Chengdu (resp. Xi'an), where the anomalous ratios for Chengdu and Xi'an are estimated as $3,930/558,098 = 0.7\%$ and $2,368/163,027 = 1.5\%$, respectively. The statistics of the datasets are reported in Table II.

Baseline. We review the literature thoroughly, and identify the following baselines for the online detection problem, including IBOAT [8], DBTOD [9], GM-VSAE [11], SD-VSAE [11], SAE [11], VSAE [11] and CTSS [10]. The detailed description of these algorithms are represented as follows:

- **IBOAT** [8]: it is an online method to detect anomalous trajectories via checking which parts of trajectories isolate from reference (i.e., normal) trajectories for the same source and destination routes.
- **DBTOD** [9]: it utilizes a probabilistic model to perform anomalous trajectory detection by modeling human driving behaviors from historical trajectories.
- **GM-VSAE** [11]: it is a method aiming to detect anomalous trajectories via a generation scheme. This method utilizes the Gaussian mixture distribution to represent categories of different normal routes. Then based on these representations, the model detects anomalous trajectories which are not well-generated.
- **SD-VSAE** [11]: it is a fast version of GM-VSAE, which outputs one representation of the normal route with the maximized probability. And based on this normal route representation, the model detects anomalous trajectories that cannot be generated well followed by GM-VSAE.

²<https://outreach.didichuxing.com/research/opendata/en/>

³<https://www.openstreetmap.org/>

- **SAE** [11]: we adapt GM-VSAE, where SAE replaces the encoder and decoder structure in GM-VSAE with a traditional Seq2Seq model, which aims to minimize a reconstruction error, and the reconstruction error is further used to define the anomaly score.
- **VSAE** [11]: we also adapt GM-VSAE by using VSAE to replace the Gaussian mixture distribution of the latent route representations in GM-VSAE with a Gaussian distribution.
- **CTSS** [10]: it is a method to detect anomalous trajectories via calculating the trajectory similarity with discrete Frechet distance between a given reference route and the current partial route at each timestamp.

We notice the baselines [9], [11], [10] are proposed for anomalous trajectory detection, and output an anomaly score on each point in a trajectory. We note that those scores are computed from the beginning, i.e., they only consider the subtrajectories starting from the source, which causes them difficult to be adapted for the subtrajectory detection task, where the detected subtrajectories can be started at any position of the trajectory. Thus, we adapt them in this way. We tune their thresholds of the anomaly scores in a development set (i.e., a set of 100 trajectories with manual labels), and for each tuned threshold, the anomalous subtrajectories are identified as those road segments, whose anomaly scores are larger than the threshold. The threshold that is associated with the best performance (evaluated by F_1 -score and details will be presented later) is selected for experiments. In addition, we also tune the parameters of baselines to the best based on the development set. For RL4OASD, it naturally outputs the anomalous subtrajectories for experiments.

Parameter Setting. In RSRNet, we embed the TCF and NRF features into the 128-dimensional vectors, and use the LSTM with 128 hidden units to implement the RSRNet. The parameter α , δ and D are set to 0.5, 0.4 and 8, respectively. To train RSRNet, we compute noisy labels in 24 time slots with one hour granularity via empirical studies. In ASDNet, the dimension of label vectors $\mathbf{v}(e_i.l)$ is 128. The policy network is implemented with a single-layer feedforward neural network, and the softmax function is adopted as the activation function. By empirical findings, the learning rates for RSRNet and ASDNet are set to 0.01 and 0.001, respectively.

Evaluation Metrics. To verify the results of subtrajectory detection, we consider two evaluation metrics. First, we adapt the evaluation metric F_1 -score proposed for Named Entity Recognition (NER) [37], [38]. This is inspired by the fact that our task corresponds to one of tagging subsequences of a sequence, which is similar to NER, which tags phrases (i.e., subsequences) of a sentence (sequence). The intuition is that we take the anomalous subtrajectories as entities in NER task. Specifically, (1) let $C_{g,i}$ denote a manually labeled anomalous subtrajectory i in the ground truth set C_g , and $C_{o,i}$ denotes the corresponding subtrajectory i in the set C_o , which is returned by a detection method. We employ Jaccard to measure the ratio of intersection over union of the road segments between $C_{g,i}$ and $C_{o,i}$. (2) We then measure the

similarity between C_g and C_o by aggregating the Jaccard $\mathcal{J}_i(C_{g,i}, C_{o,i})$.

$$\mathcal{J}_i(C_{g,i}, C_{o,i}) = \frac{|C_{g,i} \cap C_{o,i}|}{|C_{g,i} \cup C_{o,i}|}, \quad \mathcal{J}(C_g, C_o) = \sum_{i=1}^{|C_g|} \mathcal{J}_i(C_{g,i}, C_{o,i}). \quad (6)$$

Note that the intersection and union operations between $C_{g,i}$ and $C_{o,i}$ are based on 1's of the road segments of the manually labeled anomalous trajectory i . (3) Finally, we define the precision (P) and recall (R) by following [37], [38], and compute the F_1 -score accordingly.

$$P = \frac{\mathcal{J}(C_g, C_o)}{|C_o|}, \quad R = \frac{\mathcal{J}(C_g, C_o)}{|C_g|}, \quad F_1 = 2 \times \frac{P \times R}{P + R}. \quad (7)$$

Second, we further design a variant of F_1 -score. Specifically, we re-define the Jaccard similarity $\mathcal{J}_i(C_{g,i}, C_{o,i})$ to be 1 if it is above a threshold ϕ and 0 otherwise. Then, we compute the F_1 -score by Equation 7 based on the re-defined Jaccard similarity. We call this variant of F_1 -score TF_1 -score, where the threshold ϕ is naturally set to 0.5 in this paper. The intuition of TF_1 -score is to count only those detected anomalous subtrajectories which are aligned with real anomalous subtrajectories sufficiently.

Evaluation Platform. We implement RL4OASD and other baselines in Python 3.6 and Tensorflow 1.8.0. The experiments are conducted on a server with 10-cores of Intel(R) Core(TM) i9-9820X CPU @ 3.30GHz 64.0GB RAM and one Nvidia GeForce RTX 2080 GPU. The labeled datasets and codes can be downloaded via the link ⁴ to reproduce our work.

B. Effectiveness Evaluation

Comparison with existing baselines. We study the anomalous subtrajectory detection with our labeled datasets. In Table III, we report the effectiveness in terms of different trajectory lengths, e.g., we manually partition the Chengdu dataset into four groups, i.e., $G1$, $G2$, $G3$ and $G4$, such that the lengths in a groups are $G1 < 15$, $15 \leq G2 < 30$, $30 \leq G3 < 45$ and $G4 \geq 45$. We also report the overall effectiveness in whole datasets. The results clearly show that RL4OASD consistently outperforms baselines in terms of different settings. Specifically, it outperforms the best baseline (i.e., CTSS) for around 20% and 15% (resp. 30% and 28%) in terms of F_1 -score and TF_1 -score in Chengdu (resp. Xi'an) regarding the overall effectiveness, and the improvement is around 5%-26% and 1%-19% (resp. 26%-47% and 22%-45%) in terms of F_1 -score and TF_1 -score in Chengdu (resp. Xi'an) for different groups. A possible reason is that CTSS needs a threshold to extract those anomalous parts with the anomaly scores larger than the threshold. However, the threshold is hard to set appropriately for all complex traffic cases. RL4OASD demonstrates its superiority, which is mainly due to its data-driven nature for the anomalous subtrajectory detection task. Besides, we observe that RL4OASD performs

⁴<https://www.dropbox.com/sh/imix3otoep49v0g/AACQLPpgA0jMdTg7LV-GdL70a?dl=0>

TABLE III
EFFECTIVENESS COMPARISON WITH EXISTING BASELINES (LEFT: F_1 -SCORE, RIGHT: TF_1 -SCORE).

Methods	Chengdu										Xi'an									
	G1		G2		G3		G4		Overall		G1		G2		G3		G4		Overall	
IBOAT [8]	0.534	0.541	0.538	0.544	0.519	0.525	0.674	0.781	0.539	0.550	0.556	0.615	0.493	0.495	0.497	0.548	0.493	0.463	0.506	0.519
DBTOD [9]	0.523	0.533	0.531	0.537	0.515	0.522	0.669	0.750	0.530	0.542	0.519	0.523	0.448	0.381	0.441	0.380	0.483	0.452	0.433	0.424
GM-VSAE [11]	0.375	0.383	0.493	0.498	0.507	0.513	0.669	0.750	0.452	0.461	0.270	0.272	0.361	0.308	0.389	0.332	0.421	0.388	0.363	0.328
SD-VSAE [11]	0.375	0.383	0.463	0.466	0.416	0.406	0.555	0.612	0.452	0.461	0.270	0.272	0.353	0.300	0.385	0.329	0.386	0.360	0.350	0.319
SAE [11]	0.375	0.383	0.461	0.463	0.413	0.406	0.536	0.603	0.451	0.461	0.270	0.272	0.359	0.300	0.386	0.329	0.410	0.379	0.363	0.328
VSAE [11]	0.375	0.383	0.491	0.496	0.493	0.497	0.655	0.734	0.448	0.457	0.262	0.265	0.340	0.296	0.371	0.316	0.369	0.345	0.339	0.309
CTSS [10]	0.730	0.786	0.708	0.764	0.625	0.657	0.741	0.845	0.706	0.758	0.657	0.669	0.637	0.688	0.636	0.689	0.672	0.700	0.658	0.689
RL4OASD	0.888	0.905	0.892	0.910	0.725	0.720	0.774	0.853	0.854	0.870	0.964	0.973	0.864	0.888	0.809	0.843	0.844	0.870	0.857	0.883

TABLE IV
ABLATION STUDY FOR RL4OASD.

Effectiveness	F_1 -score
RL4OASD	0.854
w/o noisy labels	0.626
w/o road segment embeddings	0.828
w/o RNEL	0.816
w/o DL	0.737
w/o local reward	0.850
w/o global reward	0.849
w/o ASDNet	0.508
only transition frequency	0.643

similar trends of results in terms of F_1 -score and TF_1 -score, which shows the genericity of our method.

Ablation study. We conduct an ablation study to show the effects of some components in RL4OASD, including (1) the noisy labels, (2) pre-trained road segment embeddings, (3) Road Network Enhanced Labeling (RNEL), (4) Delayed Labeling (DL), (5) local reward, (6) global reward, (7) ASDNet and (8) transition frequency. In particular, for (1), we replace the noisy labels with random labels; for (2), we randomly initialize the embeddings of road segments to replace the pre-trained embeddings provided by Toast [33]; for (3), we drop the RNEL, and the model needs to take the action at each road segment without being guided by road networks; for (4), we drop the DL, and no delay mechanism is involved for labeling road segments; for (5), we drop the local reward, which encourages the continuity of refined labels; for (6), we drop the global reward, which provides some feedback indicating the quality of refined labels; for (7), we replace ASDNet with an ordinary classifier to follow the outputs of RSRNet, and train the classifier with noisy labels; for (8), we only use the transition frequency to detect anomalous subtrajectories, which can be regarded as the simplest method.

In Table IV, we observe each component benefits the overall effectiveness, where the ASDNet contributes quite much, because it is utilized to refine the labels which are utilized to train the RSRNet, and find out the anomalous subtrajectories. Besides, we note that (1) noisy labels, (4) Delayed Labeling (DL) and (8) transition frequency also contribute much to the performance of RL4OASD. As the aforementioned, noisy labels provide a necessary warm-start before the training with the improvement of around 36%, the delayed labeling provides the continuity of anomalous subtrajectories with the improvement of around 16%, and if we only use the transition frequency for the detection task, the performance degrades

a lot by around 25%. In addition, we also verify the effect of (2) pre-trained road segment embeddings, (3) RNEL, (5) local reward and (6) global reward. From Table IV, we observe that road segment embeddings benefit the overall effectiveness by providing the traffic context from road networks, and local reward and global reward provide some feedback signals, which guide the training of RSRNet to further provide better states for ASDNet. In addition, with the RNEL, we notice an effectiveness improvement of around 5%, since it simplifies the cases of making decisions and the model becomes easier to train.

TABLE V
IMPACTS OF PARAMETER α FOR RL4OASD.

Parameter	$\alpha = 0.3$	$\alpha = 0.4$	$\alpha = 0.5$	$\alpha = 0.6$	$\alpha = 0.7$
F_1 -score	0.844	0.845	0.854	0.846	0.845

TABLE VI
IMPACTS OF PARAMETER δ FOR RL4OASD.

Parameter	$\delta = 0.1$	$\delta = 0.2$	$\delta = 0.3$	$\delta = 0.4$	$\delta = 0.5$
F_1 -score	0.647	0.834	0.846	0.854	0.847

TABLE VII
IMPACTS OF PARAMETER D FOR RL4OASD.

Parameter	$D = 0$	$D = 2$	$D = 4$	$D = 6$	$D = 8$	$D = 10$
F_1 -score	0.737	0.763	0.812	0.833	0.854	0.848

C. Parameter Study

Varying parameter α . Table V shows the effects of varying parameter α for constructing noisy labels for training RL4OASD. Intuitively, both smaller or larger α will affect the quality of noisy labels, and lead to the model performance degradation. Specifically, the noisy labels are used in the procedure of pre-training, which provides a warm-start for the two networks, and leads to the two networks having incorporated some information of normal routes before the joint training. With a smaller α , the noisy labels are prone to 0, which affects the capability of detecting anomalous roads and vice versa. We study the parameter with the labeled Chengdu dataset. As expected, we observe its performance becomes better as α increases, and drops as the α further increases. When $\alpha = 0.5$, RL4OASD achieves the best F_1 -score.

Varying parameter δ . In Table VI, we further study the effects of varying parameter δ , where the δ controls the number of normal routes that will be selected for constructing normal route features. With a smaller δ , many existing anomalous routes in the datasets will be falsely selected as normal routes. With a larger δ , only a few normal routes will be considered, and thus some potential normal routes

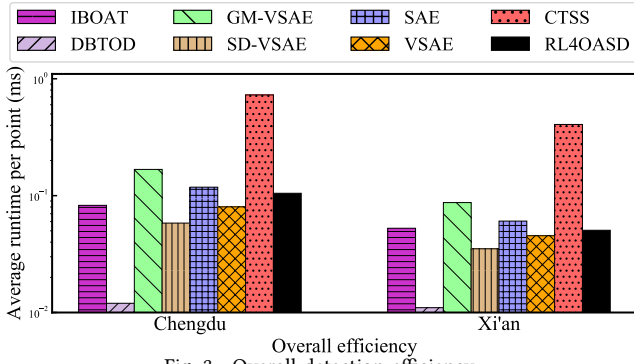


Fig. 3. Overall detection efficiency.

are missed, e.g., when δ is set to 0.5, only one route (i.e., the most frequent route) will be selected as the normal route. As expected, a moderate setting of $\delta = 0.4$ provides a balance of recognizing the number of normal routes, and contributes to the best effectiveness.

Varying parameter D . The parameter D controls the number of road segments in the delaying mechanism in order to form longer subtrajectories instead of short fragments. When $D = 0$, it reduces to the case of no delaying mechanism. The results of varying D are reported in Table VII. We observe the model performance improves as D grows, since a larger D provides better continuity of detected subtrajectories. However, with a larger D , the capability of the model to detect multiple anomalous subtrajectories will degrade, which is as expected. From Table VII, we observe that a moderate setting of $D = 8$ leads to the best effectiveness.

D. Efficiency Study

Overall detection. Figure 3 reports the online detection efficiency in terms of average running time per point on both Chengdu and Xi'an datasets. We provide the detailed analysis as follows.

We observe the running time in Chengdu is larger than in Xi'an, because the trajectories are generally shorter in Xi'an. We observe DBTOD runs the fastest on both datasets, because it is a light model with low-dimensional embeddings of some cheaper features such as road-level and turning angle for the detection, which can be accomplished very quickly, while RL4OASD involves more operations, including an LSTM-based RSRNet to capture features, and an RL-based ASDNet to label each road segment. CTSS runs the slowest since it involves discrete Frechet distance to compute the deviation between a target trajectory and a given reference trajectory, which suffers from a quadratic time complexity. In addition, for four learning-based methods GM-VSAE, SD-VSAE, SAE and VSAE that are proposed for trajectory detection via the generation scheme, we observe SD-VSAE and VSAE are generally faster than the others (i.e., GM-VSAE and SAE). This is because SAE is proposed with a traditional Seq2Seq structure, where it involves the operations of encoding and decoding, which needs to scan a trajectory twice. Compared with SAE, VSAE is free of the encoding step, and only involves the decoding step to detect some possible anomalies.

For SD-VSAE, it is a fast version of GM-VSAE, where it only predicts one Gaussian component in the encoding (or inference) step with its SD module; however, GM-VSAE needs several components in the encoding step, and uses all of them to detect anomalies in the decoding. The results are consistent with the findings that are reported in [11]. Overall, RL4OASD runs reasonably fast and would meet the practical needs, e.g., it takes less than 0.1ms to process each point, which is 20,000 times faster than the practical sampling rate of the trajectory data (2s).

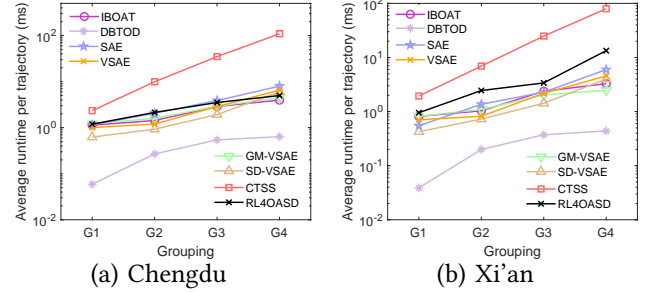


Fig. 4. Detection scalability.

Detection scalability. Further, we study the scalability for detecting ongoing trajectories in terms of four trajectory groups with different lengths. In Figure 4, we report the average running time per trajectory on both datasets. We observe the CTSS runs slowest, and its disparity between others becomes larger as the trajectory length increases. This is because CTSS involves the trajectory similarity with discrete Frechet distance to detect possible anomalies, the trend is consistent with its time complexity. DBTOD is a light model, which consistently runs the fastest. However, in terms of the effectiveness comparison reported in Table III, we note that DBTOD is not a good model for the subtrajectory detection task, though it runs faster than RL4OASD. In general, RL4OASD shows similar trends as others, and scales well with the trajectory length grows. This is because RL4OASD involves the graph structure of road networks for labeling road segments (i.e., RNEL), and the time of taking actions can be saved accordingly.

E. Case Study

In Figure 5, we investigate four representative detour cases in Chengdu, including the cases of two detours and a single detour in a target trajectory. We visualize with the green lines the detours labeled as/by Ground truth, CTSS and RL4OASD. Here, we choose CTSS for comparison, since it shows the best effectiveness among baselines. The detailed analysis is provided as follows. For the first case in Figure 5 (a)-(c), it illustrates the case of two detours in a route, we observe RL4OASD detects the detours accurately with F_1 -score=1.0; however, CTSS fails to detect the starting position of the detection. This is because CTSS measures the trajectory similarity via Frechet distance between the normal trajectory (blue) and the current ongoing trajectory (red) at each timestamp, where a detour may already happen though the ongoing trajectory is still similar to the reference

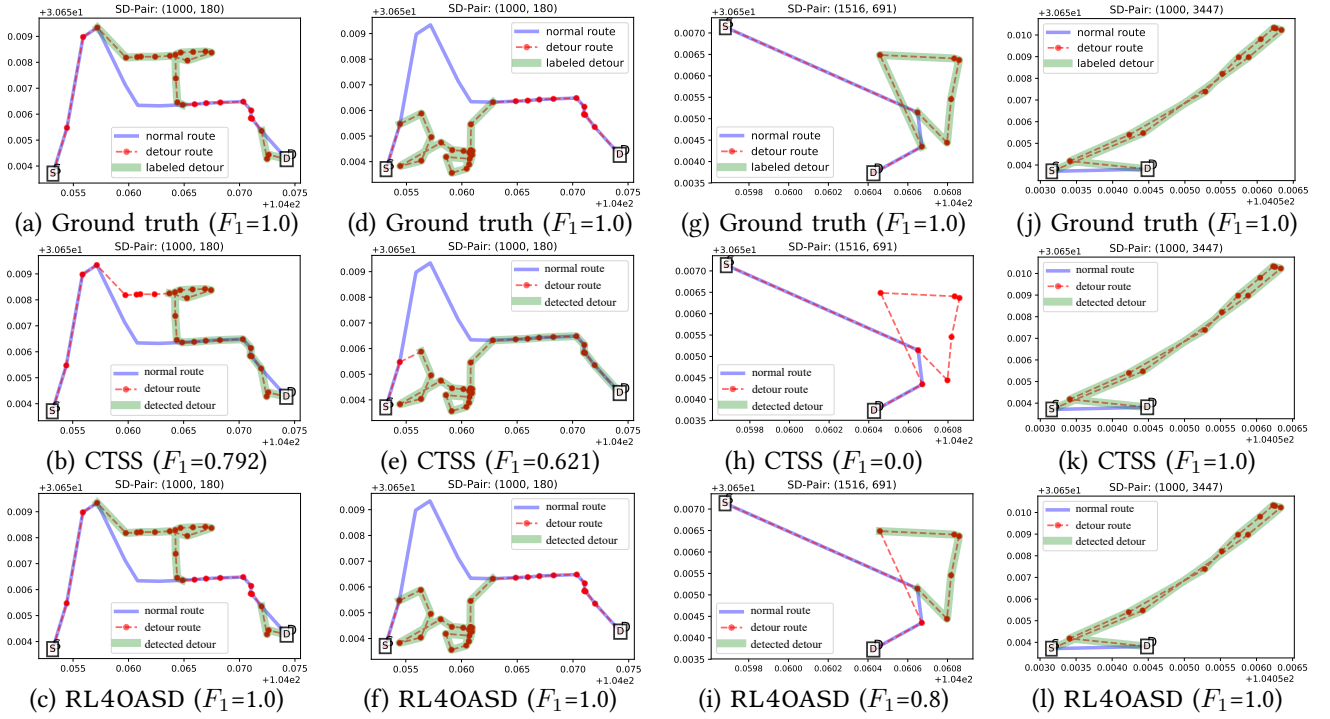


Fig. 5. Case study, blue lines: the normal routes traveled by most of trajectories; red dashed lines: the routes contained anomalous subtrajectories; red points: the intersections on road networks; green lines: the detected anomalous subtrajectories.

TABLE VIII

PREPROCESSING AND TRAINING TIME, THE MAP MATCHING [31] IS IMPLEMENTED IN C++, NOISY LABELING AND TRAINING ARE IMPLEMENTED IN PYTHON.

Data size		4,000	6,000	8,000	10,000	12,000
Preprocessing time	Map matching (s)	15.82	23.17	30.41	39.95	48.74
	Noisy labeling (s)	20.31	28.40	36.25	41.21	46.82
Training time (hours)		0.10	0.14	0.17	0.21	0.25
F_1 -score		0.723	0.786	0.821	0.854	0.854

at several starting positions. A similar case can be observed in Figure 5 (d)-(f), where CTSS detects an obvious detour with F_1 -score=0.621 only. For the case in Figure 5 (g)-(i), we observe that no detour is returned by CTSS, because CTSS employs a threshold based method to detect detours, where it reports a detour if the deviation of the current ongoing trajectory from the normal trajectory exceeds the threshold, but the threshold is hard to set appropriately and it fails in this case. For the final case in Figure 5 (j)-(l), the long detour is obvious between the source and destination, and all methods detect it accurately with F_1 -score=1.0. The results clearly show that RL4OASD can accurately identify detours, which are close to the ground truth and the returned detours are in line with human intuition. It demonstrates the capability of RL4OASD for real applications.

F. Preprocessing and Training Time

With the default setup in Section V-A, we study the preprocessing time (i.e., map-matching and noisy labeling) and training time of RL4OASD in Table VIII, by varying the data size from 4,000 trajectories to 12,000 trajectories, and

report the time costs and corresponding F_1 -scores. Overall, it takes less than two minutes in the preprocessing and around 0.2 hours to obtain a satisfactory model, and the scale is linear with the data size, which indicates the capability of RL4OASD to handle large-scale trajectory data. Here, we choose 10,000 trajectories to train RL4OASD, since it provides a reasonable trade-off between effectiveness and training time cost.

G. Detection in Varying Traffic Conditions

By following the setting in [11], we first sort the trajectories by their starting timestamps within one day, and split all the sorted trajectories into ξ partitions. For example, when ξ is set 4, we would have 4 parts within one day from Part 1 (i.e., 00:00 - 06:00, the earliest) to Part 4 (i.e., 18:00 - 24:00, the latest). Here, we consider two models, namely RL4OASD-P1 and RL4OASD-FT, to show the effectiveness of our online learning strategy for the varying traffic conditions. For RL4OASD-P1, we train it on Part 1 and directly apply it to all parts. For RL4OASD-FT, we train it on Part 1, and keep updating it (i.e., fine-tuning using stochastic gradient descent) for other parts.

We first study how to set a proper ξ . We vary the ξ from 1 to 24, and the average F_1 -scores over all parts and the corresponding training times are reported in Figure 6(a) and (b), respectively. We observe that the performance fluctuates as ξ increases, and the corresponding training time decreases because with more data parts, the size of training data for each part becomes less. We choose the $\xi = 8$, since it leads to the best effectiveness (i.e., F_1 -score=0.867) with the average

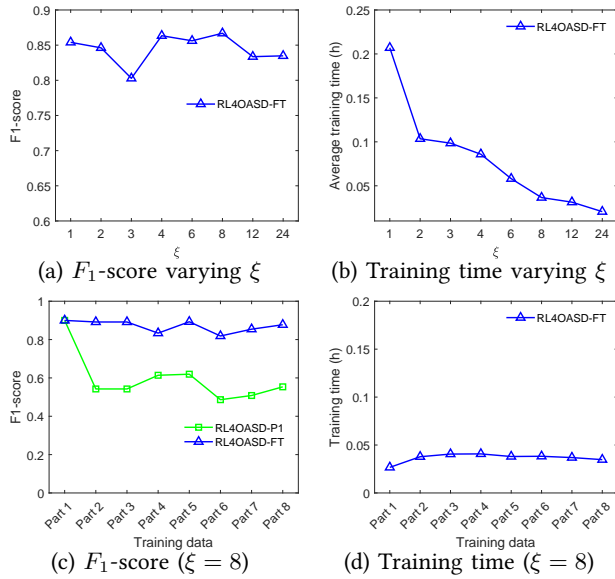


Fig. 6. Comparing RL4OASD with or without fine-tuning on newly recorded data and the corresponding training time.

training time below 0.04 hours, which is much smaller than the duration of a time period (i.e., $24/8 = 3$ hours).

With the setting of $\xi = 8$, we further compare RL4OASD-FT with RL4OASD-P1, and report the F_1 -score for each part in Figure 6(c). We observe that the performance of RL4OASD-P1 degrades on Part 2–7, which can be attributed to the concept drift. In contrast, RL4OASD-FT can improve the performance when new trajectories are being recorded to train. Therefore, our online learning strategy can easily tackle the issue of concept drift. In addition, our model is also able to handle situations with the traffic condition updated very frequently (e.g., hourly) by training from the newly recorded trajectory data. To see this, we report the training time for each part in Figure 6(d). It normally takes below 0.05 hours to update the model for each part, which largely meets the practical needs (e.g., far below the duration of each time period).

We also conduct a case study to illustrate the effectiveness of RL4OASD-FT in Figure 7. We observe the normal route and anomalous route are exchanged from Part 1 to Part 2. With the online learning strategy, RL4OASD-FT can still detect the detour on Part 2 with F_1 -score=1.0; however, RL4OASD-P1 causes the false-positive in Figure 7(c), because its policy is only trained on Part 1.

H. Cold-start problem with insufficient historical trajectories

We study the effect of cold-start problem, where we vary the number of historical trajectories within the SD pairs with a drop rate parameter. For example, if the drop rate is set to 0.2, we randomly remove 20% trajectories for the SD pairs, and the corresponding results are reported in Table IX. We observe that the effectiveness of RL4OASD is not affected by the cold-start problem much. For example, the model only degrades by 6% when 80% of historical trajectories are removed. This is possibly because the normal route feature

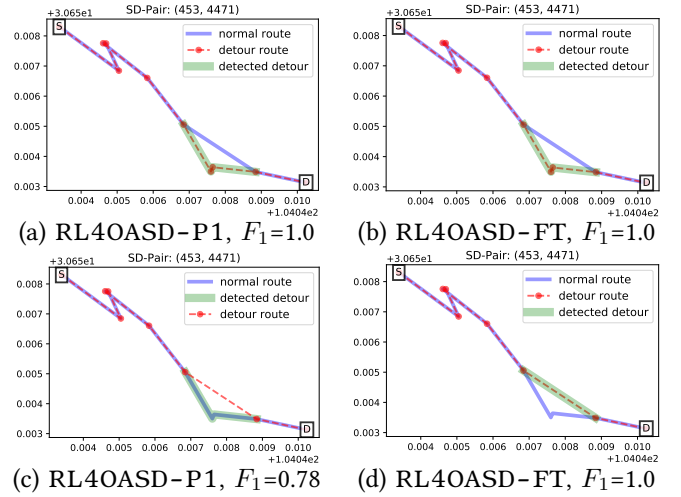


Fig. 7. Illustrating concept drift by RL4OASD-FT, where (a)-(b) for Part 1 and (c)-(d) for Part 2.

is computed in a relative way (e.g., by a fraction between 0 and 1), and the normal routes can still be identified when only few trajectories within a SD pair are available.

TABLE IX
COLD-START PROBLEM IN RL4OASD.

Drop rate	0.0	0.2	0.4	0.6	0.8
F_1 -score	0.854	0.854	0.852	0.831	0.803

VI. CONCLUSIONS

In this paper, we study the problem of online anomalous subtrajectory detection on road networks and propose the first deep reinforcement learning based solution called RL4OASD. RL4OASD is a data-driven approach that can be trained without labeled data. We conduct extensive experiments on two real-world taxi trajectory datasets with manually labeled anomalies. The results demonstrate that RL4OASD consistently outperforms existing algorithms, and runs comparably fast. In addition, RL4OASD is able to incorporate the online learning strategy to support the detection in varying traffic conditions. In the future, we will explore the subtrajectory anomaly detection task in an offline scenario, where the whole trajectory is accessible during the detection process. Another interesting direction for future research is to explore the cold-start problem when the historical trajectories are not sufficient.

REFERENCES

- [1] H. Yuan, G. Li, Z. Bao, and L. Feng, "An effective joint prediction model for travel demands and traffic flows," in *ICDE*. IEEE, 2021, pp. 348–359.
- [2] S. Feng, L. V. Tran, G. Cong, L. Chen, J. Li, and F. Li, "Hme: A hyperbolic metric embedding approach for next-poi recommendation," in *SIGIR*, 2020, pp. 1429–1438.
- [3] T. Seemann, C. R. Lane, N. L. Sherry, S. Duchene, A. Gonçalves da Silva, L. Caly, M. Sait, S. A. Ballard, K. Horan, M. B. Schultz *et al.*, "Tracking the covid-19 pandemic in australia using genomics," *Nature communications*, vol. 11, no. 1, pp. 1–9, 2020.
- [4] C. Huang, J. Zhang, Y. Zheng, and N. V. Chawla, "Deepcrime: Attentive hierarchical recurrent networks for crime prediction," in *CIKM*, 2018, pp. 1423–1432.

- [5] Z. Yuan, X. Zhou, and T. Yang, "Hetero-convlstm: A deep learning approach to traffic accident prediction on heterogeneous spatio-temporal data," in *KDD*, 2018, pp. 984–992.
- [6] Y. Ning, L. Zhao, F. Chen, C.-T. Lu, and H. Rangwala, "Spatio-temporal event forecasting and precursor identification," in *KDD*, 2019, pp. 3237–3238.
- [7] C. Chen, D. Zhang, P. S. Castro, N. Li, L. Sun, and S. Li, "Real-time detection of anomalous taxi trajectories from gps traces," in *International Conference on Mobile and Ubiquitous Systems: Computing, Networking, and Services*. Springer, 2011, pp. 63–74.
- [8] C. Chen, D. Zhang, P. S. Castro, N. Li, L. Sun, S. Li, and Z. Wang, "iboat: Isolation-based online anomalous trajectory detection," *IEEE Transactions on Intelligent Transportation Systems*, vol. 14, no. 2, pp. 806–818, 2013.
- [9] H. Wu, W. Sun, and B. Zheng, "A fast trajectory outlier detection approach via driving behavior modeling," in *Proceedings of the 2017 ACM Conference on Information and Knowledge Management*, 2017, pp. 837–846.
- [10] D. Zhang, Z. Chang, S. Wu, Y. Yuan, K.-L. Tan, and G. Chen, "Continuous trajectory similarity search for online outlier detection," *IEEE Transactions on Knowledge and Data Engineering*, 2020.
- [11] Y. Liu, K. Zhao, G. Cong, and Z. Bao, "Online anomalous trajectory detection with deep generative sequence modeling," in *2020 IEEE 36th International Conference on Data Engineering (ICDE)*. IEEE, 2020, pp. 949–960.
- [12] L. Song, R. Wang, D. Xiao, X. Han, Y. Cai, and C. Shi, "Anomalous trajectory detection using recurrent neural network," in *International Conference on Advanced Data Mining and Applications*. Springer, 2018, pp. 263–277.
- [13] X. Li, J. Han, S. Kim, and H. Gonzalez, "Roam: Rule-and motif-based anomaly detection in massive moving object data sets," in *Proceedings of the 2007 SIAM International Conference on Data Mining*. SIAM, 2007, pp. 273–284.
- [14] D. Silver, G. Lever, N. Heess, T. Degris, D. Wierstra, and M. Riedmiller, "Deterministic policy gradient algorithms," in *International conference on machine learning*. PMLR, 2014, pp. 387–395.
- [15] J.-G. Lee, J. Han, and X. Li, "Trajectory outlier detection: A partition-and-detect framework," in *2008 IEEE 24th International Conference on Data Engineering*. IEEE, 2008, pp. 140–149.
- [16] D. Zhang, N. Li, Z.-H. Zhou, C. Chen, L. Sun, and S. Li, "ibat: detecting anomalous taxi trajectories from gps traces," in *Proceedings of the 13th international conference on Ubiquitous computing*, 2011, pp. 99–108.
- [17] J. Zhu, W. Jiang, A. Liu, G. Liu, and L. Zhao, "Time-dependent popular routes based trajectory outlier detection," in *International Conference on Web Information Systems Engineering*. Springer, 2015, pp. 16–30.
- [18] Z. Lv, J. Xu, P. Zhao, G. Liu, L. Zhao, and X. Zhou, "Outlier trajectory detection: A trajectory analytics based approach," in *International Conference on Database Systems for Advanced Applications*. Springer, 2017, pp. 231–246.
- [19] P. Banerjee, P. Yawalkar, and S. Ranu, "Mantra: a scalable approach to mining temporally anomalous sub-trajectories," in *Proceedings of the 22nd ACM SIGKDD International Conference on Knowledge Discovery and Data Mining*, 2016, pp. 1415–1424.
- [20] K. Gray, D. Smolyak, S. Badirli, and G. Mohler, "Coupled igmm-gans for deep multimodal anomaly detection in human mobility data," *arXiv preprint arXiv:1809.02728*, 2018.
- [21] Y. Ge, H. Xiong, C. Liu, and Z.-H. Zhou, "A taxi driving fraud detection system," in *2011 IEEE 11th International Conference on Data Mining*. IEEE, 2011, pp. 181–190.
- [22] X. Li, Z. Li, J. Han, and J.-G. Lee, "Temporal outlier detection in vehicle traffic data," in *2009 IEEE 25th International Conference on Data Engineering*. IEEE, 2009, pp. 1319–1322.
- [23] Y. Ge, H. Xiong, Z.-h. Zhou, H. Ozdemir, J. Yu, and K. C. Lee, "Top-eye: Top-k evolving trajectory outlier detection," in *Proceedings of the 19th ACM international conference on Information and knowledge management*, 2010, pp. 1733–1736.
- [24] Y. Yu, L. Cao, E. A. Rundensteiner, and Q. Wang, "Detecting moving object outliers in massive-scale trajectory streams," in *Proceedings of the 20th ACM SIGKDD international conference on Knowledge discovery and data mining*, 2014, pp. 422–431.
- [25] R. S. Sutton and A. G. Barto, *Reinforcement learning: An introduction*. MIT press, 2018.
- [26] M. L. Puterman, *Markov decision processes: discrete stochastic dynamic programming*. John Wiley & Sons, 2014.
- [27] M.-h. Oh and G. Iyengar, "Sequential anomaly detection using inverse reinforcement learning," in *Proceedings of the 25th ACM SIGKDD International Conference on Knowledge Discovery & data mining*, 2019, pp. 1480–1490.
- [28] C. Huang, Y. Wu, Y. Zuo, K. Pei, and G. Min, "Towards experienced anomaly detector through reinforcement learning," in *Thirty-Second AAAI Conference on Artificial Intelligence*, 2018.
- [29] Z. Wang, C. Long, G. Cong, and Y. Liu, "Efficient and effective similar subtrajectory search with deep reinforcement learning," *Proceedings of the VLDB Endowment*, vol. 13, no. 12, pp. 2312–2325, 2020.
- [30] R. S. Sutton, D. A. McAllester, S. P. Singh, and Y. Mansour, "Policy gradient methods for reinforcement learning with function approximation," in *Advances in neural information processing systems*, 2000, pp. 1057–1063.
- [31] C. Yang and G. Gidofalvi, "Fast map matching, an algorithm integrating hidden markov model with precomputation," *IJGIS*, vol. 32, no. 3, pp. 547–570, 2018.
- [32] S. Hochreiter and J. Schmidhuber, "Long short-term memory," *Neural computation*, vol. 9, no. 8, pp. 1735–1780, 1997.
- [33] Y. Chen, X. Li, G. Cong, Z. Bao, C. Long, Y. Liu, A. Chandran, and R. Ellison, "Robust road network representation learning: When traffic patterns meet traveling semantics," 2021.
- [34] T. S. Jepsen, C. S. Jensen, and T. D. Nielsen, "Graph convolutional networks for road networks," in *Proceedings of the 27th ACM SIGSPATIAL International Conference on Advances in Geographic Information Systems*, 2019, pp. 460–463.
- [35] M.-x. Wang, W.-C. Lee, T.-y. Fu, and G. Yu, "Learning embeddings of intersections on road networks," in *Proceedings of the 27th ACM SIGSPATIAL International Conference on Advances in Geographic Information Systems*, 2019, pp. 309–318.
- [36] R. J. Williams, "Simple statistical gradient-following algorithms for connectionist reinforcement learning," *Machine learning*, vol. 8, no. 3, pp. 229–256, 1992.
- [37] J. Li, A. Sun, J. Han, and C. Li, "A survey on deep learning for named entity recognition," *IEEE Transactions on Knowledge and Data Engineering*, 2020.
- [38] F. Li, Z. Wang, S. C. Hui, L. Liao, D. Song, and J. Xu, "Effective named entity recognition with boundary-aware bidirectional neural networks," in *Proceedings of the Web Conference 2021*, 2021, pp. 1695–1703.